Relaxation Dynamics of Entangled and Unentangled Multiarm Polymer Solutions: Comparisons with Theory

Juliani and Lynden A. Archer*

School of Chemical Engineering, Cornell University, Ithaca, New York 14853-5201

Received May 30, 2002

ABSTRACT: Linear viscoelastic properties of model branched $A_3-\mathbf{A}-A_3$ 1,4-polybutadiene melts and solutions are investigated experimentally, using small-amplitude oscillatory shear measurements, and theoretically, using a recent tube model theory for stress relaxation of entangled H-shaped polymers. This study provides experimental guidance on two key assumptions in the theory: namely, that stress relaxation of multiply branched, entangled polymers is hierarchical and that relaxed portions of a branched molecule accelerate stress relaxation of unrelaxed sections of the same molecule in qualitatively the same manner as a low molecular weight diluent. Experimental results for multiarm $A_3-\mathbf{A}-A_3$ polymer melts and solutions covering a wide range of arm *A* and connector **A** molecular weights provide broad support for a hierarchical relaxation process in these materials. However, linear viscoelastic data for $A_3-\mathbf{A}-A_3$ polymers strongly disagree with the second assumption. Specifically, we find that the relaxed arms provide a much greater than expected retardation of branch point motion even on time scales well beyond the arm relaxation time. Branch point diffusivities estimated from the experimental data are typically 1−2 orders of magnitude lower than predicted by theory. The theory also underpredicts the breadth and amplitude of the dynamic storage and loss moduli of multiarm melts and solutions, particularly for materials where the number of entanglements per arm is low.

Introduction

In a previous article,[1] we reported results from an experimental study of stress relaxation dynamics of model $A_3-\mathbf{A}-A_3$ multiarm, long-chain branched (LCB) 1,4-polybutadiene melts and solutions. In that study, small-amplitude oscillatory shear measurements over a broad temperature range were used to investigate liquid state dynamics arising from polymer segment librations to translation diffusion of entire branched polymer molecules. By systematically varying arm (*A*) molecular weight M_a, cross-bar **A** molecular weight M_{cb}, and multiarm polymer volume fraction ϕ, multiarm solutions possessing a broad range of arm entanglement densities (i.e., $M_a/M_e(\phi) < 1$ to $M_a/M_e(\phi) \gg 1$) were formulated to permit the effect of arm entanglements on dynamics to be determined. Here $M_e(\phi) = M_{e0}\phi^{-4/3}$ is the entanglement molecular weight in solution.

The main findings of ref 1 can be summarized as follows: (i) Stress relaxation dynamics of entangled multiarm $A_3-\mathbf{A}-A_3$ polymers appear to be hierarchical (*A* arms relax first, during which time the cross-bar **A** contribution to stress remains virtually constant). (ii) Relaxed arms dilate the entanglement network in which cross-bar segments relax in much the same way as a low molecular weight Θ solvent. It is unclear from the data, however, whether the this dilation is produced by simple constraint release (CR) of cross-bar segments by the faster relaxing arms or by a dynamic tube dilation process (DTD). (iii) Relaxed arms (entangled or unentangled) exert a surprisingly large influence on terminal dynamics well after their contribution to the total stress disappear. Thus, while multiarm solutions with $M_a/M_e(\phi) < 1$ might be anticipated to display dynamics similar to those of linear molecules with large friction centers at their ends (perhaps suppressing contour length fluctuations (CLF)), experiments indicate that the zero shear viscosity η_0 of these solutions varies with polymer volume fraction as $\eta_0 \sim \phi^{2.9\pm0.2}$ and that the longest relaxation time λ varies with ϕ as $\lambda \sim \phi^{2.6\pm0.3}$.[1] The latter dependence is much stronger than $\lambda \sim \phi^{4/3}$ expected for reptation of entangled linear-like multiarm molecules, with CLF suppressed.

$$\lambda = \frac{L_{cb}^{\,2}\zeta_{T,cb}}{3\pi^2 kT} = \tau_m\left(\frac{M_{cb}^{\,2}}{M_{e0}}\phi_{cb}^{\,4/3}\right)\left(\frac{M_{cb}}{m_0} + 2q(\tau_{arm}/\tau_m)\right) \quad (1)$$

Here $\zeta_{T,cb}$ is the Rouse tube friction coefficient of the cross-bar and includes the extra friction that arises from the $2q$ arms appended to the cross-bar, L_{cb} is the crossbar contour length, $\phi_{cb} = \phi M_{cb}/(M_{cb} + qM_a)$, m_0 is the repeat unit molecular weight, τ_{arm} is the arm relaxation time, q is the number of arms per branch point (assumed here to be symmetric based on earlier light scattering results for the unlinked arms and cross-bars and the fully linked multiarm molecules[2]), and τ_m is the segmental or monomer relaxation time.

In multiarm solutions with $M_a/M_e > 2$, our earlier experiments also yield η_0 and λ results that are much stronger functions of M_{cb} and concentration than expected from eq 1,[1]

$$\eta_0 \approx \eta_e C_1\left[\left(\frac{M_{cb}}{M_e}\right)^3 + \left(\frac{M_a}{M_e}\right)^2 \exp\left\{\nu\left(\frac{M_a}{M_e} + \frac{M_{cb}}{M_e}\right)\right\}\right] \quad (2)$$

$$\lambda \approx \tau_e C_2\left[\left(\frac{M_{cb}}{M_e}\right)^3 + \left(\frac{M_a}{M_e}\right)^2 \exp\left\{\nu\left(\frac{M_a}{M_e} + \frac{M_{cb}}{M_e}\right)\right\}\right] \quad (3)$$

Here η_e and τ_e are the Rouse viscosity and relaxation time of a network segment with molecular weight $M_e = M_e(\phi)$; $\nu = 0.42 \pm 0.06$, $C_1 = 150 \pm 50$, and $C_2 = 7000$ are empirical coefficients.[1] Though the exponential dependence of η_0 and λ on arm entanglement density is expected, the exponential dependence on cross-bar molecular weight is not.

10.1021/ma0208436 CCC: $22.00
Published on Web 12/05/2002

Table 1. Molecular Characteristics for Multiarm Polybutadiene Melts at 26 °C

sample	M_w cross-bar[a]	M_w arm[a]	M_w polymer[b]	M_w/M_n polymer	λ_e [s]	$G_N \times 10^{-6}$ [Pa]
P1184	3.87×10^4	1.46×10^4	12.8×10^4	1.15	2.88×10^{-6}	1.28
P1589	8.9×10^4	2.1×10^4	21.03×10^4	1.04	1.74×10^{-6}	1.19
P1625	13.2×10^4	2.2×10^4	26.7×10^4	1.06	1.26×10^{-6}	1.28
MA15	10.1×10^4	3.7×10^4	32.2×10^4	1.19	6.30×10^{-7}	1.49

[a] M_w cross-bar and M_w arm from SEC only. [b] Absolute M_w of multiarm polymer from SEC−multiangle laser light scattering analysis.

There are at least two physical processes by which these stronger than expected concentration and M_{cb} dependencies can be rationalized. First, one might suppose that since cross-bar segments relax on time scales substantially longer than arm relaxation times, the mechanism of dynamic dilution proposed by Ball and McLeish[3] must be modified by the presence of cross-bars.[4] Second, it is possible that even after the arms have relaxed, dilating the entanglement environment around cross-bars by CR or DTD, cross-bar segments are forced to diffuse in their original tubes until CR events between mutually entangled cross-bars release enough cross-bar constraints that the diameter of the dilated tube $a(\phi)$ approaches the total coil size $(qM_a^{1/2}/\sqrt{6m_0})b$ of the arms. In this situation, cross-bar retraction becomes competitive with reptation for relaxing stress in cross-bar segments.

Both mechanisms can be captured, approximately, using the recent theory for stress relaxation dynamics of branched polymers by McLeish and co-workers.[5] The first mechanism is accounted for in the theory by introducing a finite concentration of stationary cross-bar segments into the DTD equations for arm relaxation. The second mechanism is captured approximately by introducing a renormalized branch point diffusivity $D_{bp} = p^2a(\phi)^2/2q\tau_a$, which can be made arbitrarily small by appropriate choice of the parameter p. Here p defines the fraction of a tube diameter the branch point moves in a time of order τ_a. This parameter would be unity for motion at the ends of an entangled linear molecule, where the corresponding diffusion time is the entanglement hopping time τ_e. p can be lower than unity for branch point diffusion in a tube, however, because motion of the branch point is restricted by the tube constraints acting simultaneously on each of the q arms. A formal crossover to reptation diffusion occurs when the cross-bar reptation time given by eq 1 (adjusted for the much lower branch point diffusion coefficient) becomes comparable to the arm retraction time of cross-bar segments.[5]

In the present study we focus on comparisons between experimental results and the theory of McLeish et al.[5] for stress relaxation in branched polymers. Our overall goal is to systematically evaluate predictions of the theory for $A_3-\mathbf{A}-A_3$ branched polymer melts and solutions, by comparing model predictions with experimentally measured dynamic moduli. We are particularly interested in understanding the subtle processes by which relaxed arms simultaneously dilate the network environment in which cross-bar segments relax, yet appear to impede cross-bar dynamics in qualitatively the same manner as expected for long unrelaxed arms. Our findings may also be useful for guiding new computer simulation approaches for describing branched polymer dynamics.[6]

Experiment

Linear viscoelastic properties of multiarm polymer melts and solutions in an oligomer of 1,4-polybutadiene ($M_w = 1000$) were characterized by small-amplitude oscillatory shear rheometry. The architecture of these materials was studied by size-exclusion chromatography and light scattering, and the results have been reported previously.[1,2] These results indicate that, with minor exceptions, the targeted $A_3-\mathbf{A}-A_3$ multiarm architecture is achieved using the synthesis scheme reported by Archer and Varshney,[7] provided synthesis is followed by repeated fractionation in toluene/methanol mixtures. The microstructure of all polymers used in the study were characterized by deuterium NMR, and the results are reported in ref 1. These results support a dominantly 1,4-polybutadiene microstructure for the entire multiarm molecule.

Rheometry measurements were performed at temperatures ranging from −80 to 26 °C and the data shifted to 26 °C using time−temperature superposition. A Paar Physica modular compact rheometer (MCR300) with a CTD600 temperature controller was used for the measurements. Temperature regulation for low-temperature measurements was performed using liquid nitrogen. Stainless steel parallel plate (25 and 6 mm diameter) rheometer fixtures were used for the oscillatory shear experiments. Because of the rather long relaxation time of virtually all multiarm melts and some of the solutions used in the study, parallel plate fixtures with relatively large separations (typically 1 or 0.5 mm), and long sample loading and annealing times (typically 5−10 times the terminal time, which is of the order of a month for some materials) are required. Rheological information obtained from these experiments is summarized in Table 1 for the melts and in the previous paper (ref 1) for the solutions. The mean entanglement hopping time $\tau_e \approx \omega_e^{-1}$ was estimated from the frequency ω_e at which the plateau and high-frequency power-law ("Rouse") dynamic regimes intersect.[8] Zero shear viscosities $\eta_0 = \lim_{\omega\to 0}(G''(\omega)/\omega)$ were determined from the slope of $G''(\omega)$ in the terminal region. Terminal relaxation times λ were estimated from $\eta''(\omega)/\eta_0$ data as the inverse of the frequency ω_M where $\eta''(\omega)/\eta_0$ manifests a local maximum in the terminal zone.

Theory

As already discussed, one of our goals is to compare relaxation behavior observed experimentally in model branched polymers with a promising recent tube-model theory for branched polymer dynamics developed by McLeish and co-workers.[5] We begin with a brief review of the theory for stress relaxation dynamics in H-shaped polymer melts. The main premise of the theory is that relaxation dynamics in multiply branched entangled polymers are hierarchical (i.e., relaxation progresses from the outermost arm segments inward). Stress relaxation in an $(A_n-\mathbf{A}-A_n)$ polymer can, for example, be constructed as sequential relaxation of starlike arms and linearlike cross-bar chain segments. In the theory of McLeish et al. arm segments relax first by rapid Rouse motions at their extremities; this is followed by activated arm retraction in a dynamically dilated tube comprised of relaxing arm and unrelaxed cross-bar **A** chain segments. After arm relaxation, the junction points connecting cross-bar and arms execute Rouse-like hopping motions in a tube dilated by relaxed arm segments. Final relaxation occurs by a combination of CLF and slow reptation diffusion of cross-bar segments in the dilated tube.

Since the arm and cross-bar relaxation processes occur on very different time scales, the complex dynamic

modulus can be obtained by separate integrations over arm and cross-bar relaxation modes,[5]

$$G^*(\omega) = G_0(\alpha+1)\left[\int_0^1 dx_a\, \phi_a(1-\phi_a x_a)^\alpha \frac{i\omega\tau_a(x_a)}{1-i\omega\tau_a(x_a)} + \int_0^{x_c} dx_b\, \phi_{cb}^{\alpha+1}(1-x_b)^\alpha \frac{i\omega\lambda(x_b)}{1-i\omega\lambda(x_b)}\right] \quad (4)$$

The dilution exponent ($\alpha = {}^4/_3$) is taken to be the same as in a Θ solvent,[9] because the arm and cross-bar segments are chemically the same. Because arms and cross-bar segments relax sequentially, two separate path length variables $0 \le x_a \le 1$ and $0 \le x_b \le x_c$ are used to track the progress of relaxation in the respective sections of a multiarm molecule, i.e., from the outermost segments ($x_i = 0$) inward. The upper bound value of x_a corresponds to complete arm retraction, while the upper bound value on x_b is set by the crossover from cross-bar contour length fluctuations to reptation-dominated dynamics which occurs at the path length coordinate x_c. There are then four primary modes of relaxation in a multiarm polymer: two arm modes and two cross-bar modes. The fast arm Rouse mode and slow retraction modes can be combined to define a single composite arm relaxation time $\tau_a(x_a)$. This time depends on arm entanglement density M_a/M_e, arm volume fraction ϕ_a, and τ_e in a similar manner as for arm retraction in a concentrated solution of star polymer molecules, but with the exception that dynamic dilution by the more slowly relaxing cross-bar segments is disallowed.[5]

As pointed out earlier, the retarding effect of A arms on cross-bar diffusion can be captured by allowing the branch point diffusivity D_{bp} to depend on the new parameter p. $D_{bp} = p^2a^2/2q\tau_a$. In the case of the *H-shaped* polymer melts, McLeish et al. found that p^2 values in the range of ${}^1/_6$ to ${}^1/_{12}$ fairly described their experimental results.[5,10] Such a low p^2 value indicates that the crossover from CLF-dominated to reptation-dominated dynamics is significantly delayed in H-shaped polymers, perhaps explaining the stronger than expected dependence of terminal properties on for entangled polymers.[1]

Results and Discussion

The entanglement Rouse relaxation time τ_e is one of the three parameters needed to compare predictions of the theory of McLeish et al. to experimental results. τ_e values in the systems studied here can vary for at least two reasons. First, $\tau_e = N_e^2(\phi)\,\tau_m$ is a function of multiarm polymer concentration in solution. Second, in 1,4-polybutadienes τ_m is sensitive to the microstructure (1−2/1−4 isomer content) of the polymer, so τ_e may vary from polymer to polymer. To remove these effects, τ_e was estimated from high-frequency (low-temperature) oscillatory shear measurements as the intersection of $G'(\omega)$ in the rubbery plateau with $G'(\omega)$ in the high-frequency Rouse power-law regime. Results for all multiarm solutions used in the study are provided in Table 1. Plateau moduli used for comparisons between theory and experiment were calculated using the relation $G_N(\phi) = G_{N0}\phi^{7/3}$, where G_{N0} is the plateau modulus for the multiarm melt and the polymer volume fraction in solution. Values of G_{N0} used in the comparisons are also provided in Table 1. The entanglement molecular weight used in the calculations was likewise determined from the relation $M_e(\phi) = M_{e0}\phi^{-4/3}$, where $M_{e0} = 1822$ g/mol is the entanglement molecular weight of a dominantly 1,4-polybutadiene (>90% 1,4-) melt.

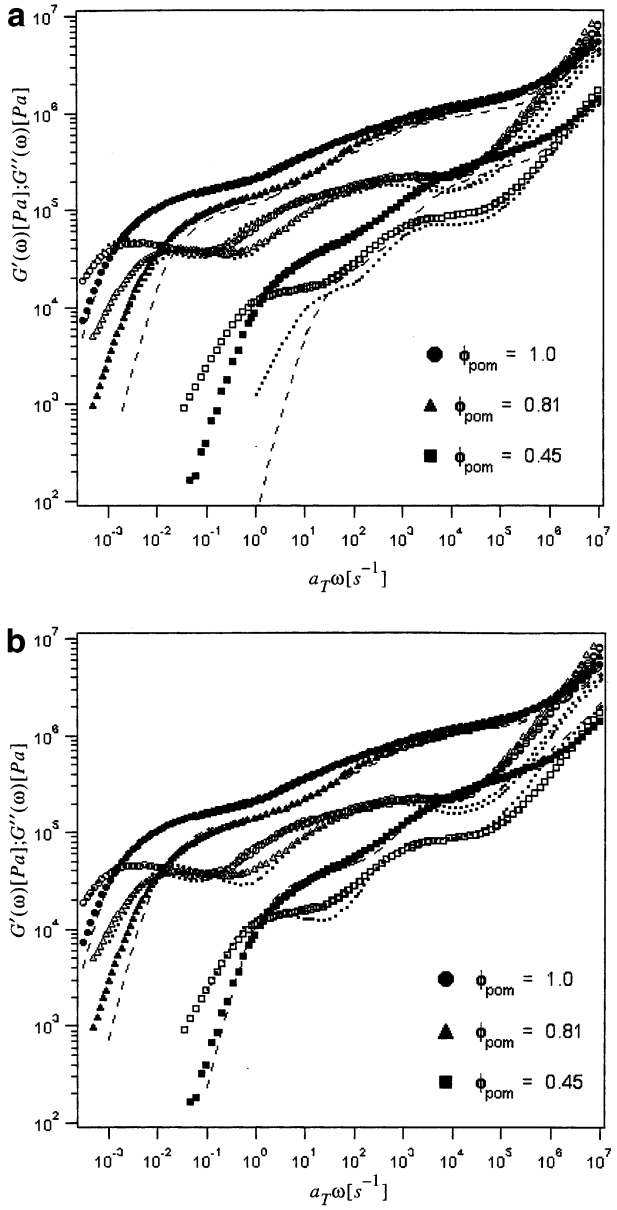

Figure 1. (**a**) Experimental $G'(\omega)$ (filled symbols) and $G''(\omega)$ (open symbols) for solutions of P1589 at 26 °C compared with theoretical predictions, $G'(\omega)$ (broken lines) and $G''(\omega)$ (dots), for various solution concentrations. A fixed value of the branch point hopping parameter, $p^2 = {}^1/_6$, is used for the theoretical analysis. (**b**) $G'(\omega)$ (filled symbols) and $G''(\omega)$ (open symbols) for solutions of P1589 compared with theoretical predictions, $G'(\omega)$ (broken lines) and $G''(\omega)$ (dots), for various solution concentrations. Branch point hopping parameters $p^2 = {}^1/_6$ for the multiarm polymer melt, $p^2 = {}^1/_{17}$ for a multiarm solution with $\phi_{pom} = 0.81$, and $p^2 = {}^1/_{58}$ for a solution with $\phi_{pom} = 0.45$ were used in the analysis.

Storage and loss moduli for P1589O_ multiarm melt and solutions are presented in Figure 1a. If relaxed arms dilute cross-bar entanglements at long times, the number of remaining cross-bar entanglements per molecule $s_{b,\tau_{arm}}$ varies from 15 in the melt to 5 in the 45% solution. The lines through the data are the predictions of the theory of McLeish et al.,[5] with $p^2 = {}^1/_6$. Except for the fact that loss moduli are underpredicted by about 15% at high frequencies, the theory captures most features of the melt behavior very well. As solution concentration is reduced, however, the

Table 2. p^2 Values for P1589O_ Series Multiarm Solutions

sample	ϕ_{P1589}	$1/p^2$	sample	ϕ_{P1589}	$1/p^2$
P1589O21	0.210	150	P1589O66	0.657	18
P1589O31	0.316	95	P1589O80	0.806	17
P1589O45	0.452	58	P1589	1.0	6

theoretical predictions are seen to deviate significantly from the experimental data over the entire frequency range. The largest discrepancies are observed at low multiarm solution concentrations. In all cases the deviations are also seen to be negative ones, indicating that P1589 solutions relax more slowly than expected from theory.

The success of the H-polymer model in describing linear viscoelastic properties of the P1589 melt appears to rule out material-related problems, such as polydispersity of the arms and/or cross-bar, as the cause of the discrepancies between theory and experiment. This behavior could arise, however, from an incorrect (too large) value of the dilution exponent in the expressions for $G_N(\phi)$ and $M_e(\phi)$. The value of $^4/_3$ used here seems to justified by the fact that polymer segments are the same as the solvent. Nonetheless, because of the low molecular weight of the PBD used as solvent, it may be argued that good solvent dilution exponents ($\beta \approx {}^5/_4$), rather than the Θ solvent value ($\beta \approx {}^4/_3$), may be more appropriate.[11] This change lowers the value of $G_N(\phi)$ and increases the value of $M_e(\phi)$ at any $\phi < 1$, which further increases the discrepancy between theoretical predictions and experimental results.

Judging from the shapes of the predicted $G'(\omega)$ and $G''(\omega)$ curves particularly at low concentration, the theory also seems to predict a much earlier transition to linear-like material response than observed experimentally. This prediction appears to result from an underestimation of the influence of mildly entangled arms on terminal dynamics of entangled branched molecules.The model of McLeish et al.[5] provides a simple mechanism for enhancing the influence of arms on terminal relaxation dynamics of H-shaped molecules. Specifically, as the branch point hopping amplitude p^2 is made progressively smaller, arm retraction becomes more competitive with reptational diffusion for relaxing stress at long times, allowing arms to exert a longer-lived influence on cross-bar dynamics than would be expected from a strictly hierarchical DTD model for stress relaxation. Figure 1b compares theoretical predictions with experimental results in the situation where p^2 is allowed to vary freely with multiarm concentration. Agreement between theory and experiment is clearly improved using this approach. However, the values of p^2 required to secure better agreement with the data are significantly lower than for the melt (see Table 2). It is also apparent from the table that p^2 is an increasing function of multiarm solution concentration. Thus, while p^2 for the P1589 multiarm melt is a factor of 2 larger than the best-fit value reported for H-polymer melts, $p^2 \approx 1/150$ for the lowest solution concentration ($\phi_{pom} = 0.2$, $s_{b,\tau_{arm}} < 2$, and $M_a/M_e = 1$). This finding is exactly opposite to what one would expect if p truly measured retardation of branch point motion by entangled arms.

The large increase in number of diffusive steps required to transport a branch point one tube diameter implies that cross-bar retraction might in fact be the preferred mechanism for relaxing stress in the cross-bar, even in $A_3-\mathbf{A}-A_3$ solutions with arm entanglement densities of order unity. This observation is consistent with our earlier finding that despite the linearlike structure of the cross-bar in $A_3-\mathbf{A}-A_3$ polymers following relaxation of A arms, terminal properties manifest starlike dependences on M_{cb}.[1] p is therefore perhaps better viewed as an empirical parameter that tunes the balance between cross-bar relaxation by arm retraction and reptation diffusion in the theory. Such a parameter is obviously undesirable in a molecular theory. More in-depth understanding of the range of values p can take in multiarm melts and solutions should nonetheless help identify what physics are needed to improve the theory.

Figure 2a,b compares $G'(\omega)$ and $G''(\omega)$ data with theoretical predictions for a multiarm polymer with lower M_a and M_{cb}. In this case, the theory with $p^2 = {}^1/_6$ underpredicts both the melt and solution data, except at high frequencies. This observation is also worrisome because it indicates that p^2 is not universal for multiarm melts with the same architecture. Figure 2b further shows that while lower p^2 values do improve the breadth of predicted relaxation spectra, the shapes of $G'(\omega)$ and $G''(\omega)$ are incorrect. Changes in the cross-bar hopping amplitude alone therefore do not entirely account for the differences between experiment and theory. Additional results for solutions of a third multiarm polymer, P1625, with arm molecular weight comparable to P1589 but with higher cross-bar molecular weights, are provided in Figure 3a. Again, clear qualitative similarities between theoretical predictions and experimental results are observed. However, in this case even a p^2 value of $^1/_{24}$ in the melt cannot capture the experimental trends. Even lower p^2 values than before are required to describe the solution results. Results for a polymer with cross-bar molecular weight comparable to P1589, but possessing larger arm molecular weights (MA15), are provided in Figure 3b. The extremely long relaxation time of this material limits melt data to a relatively narrow frequency range. Over the range of accessible frequencies, the theory appears to fairly describe relaxation dynamics of this material. However, it is again noticed that as the polymer concentration in solution is reduced, progressively larger discrepancies between theoretical predictions and experimental results are observed. The extremely low p^2 values required to correctly capture the breadth of the relaxation spectra for solutions of MA15 (Table 5) indicate that relaxation dynamics in this material are essentially starlike.

Conclusions

Linear viscoelastic behavior of multiarm polybutadiene melts and solutions are studied using oscillatory shear rheometry. Experimental storage ($G'(\omega)$) and loss ($G''(\omega)$) moduli data are compared with predictions from a recent theory by McLeish and co-workers[5] for stress relaxation of H-shaped polymers. Direct comparisons between theory and experiments using a single value of the branch point hopping parameter $p^2 = {}^1/_6$ yield theoretical predictions that are in fair accord with experimental observations for some of the materials in the melt. Serious discrepancies are observed, however, between theoretical predictions and experimental $G'(\omega)$ and $G''(\omega)$ data for all multiarm solutions and some of the multiarm melts studied. Experiments indicate that terminal relaxation of these materials is substantially slower than predicted by theory. We have

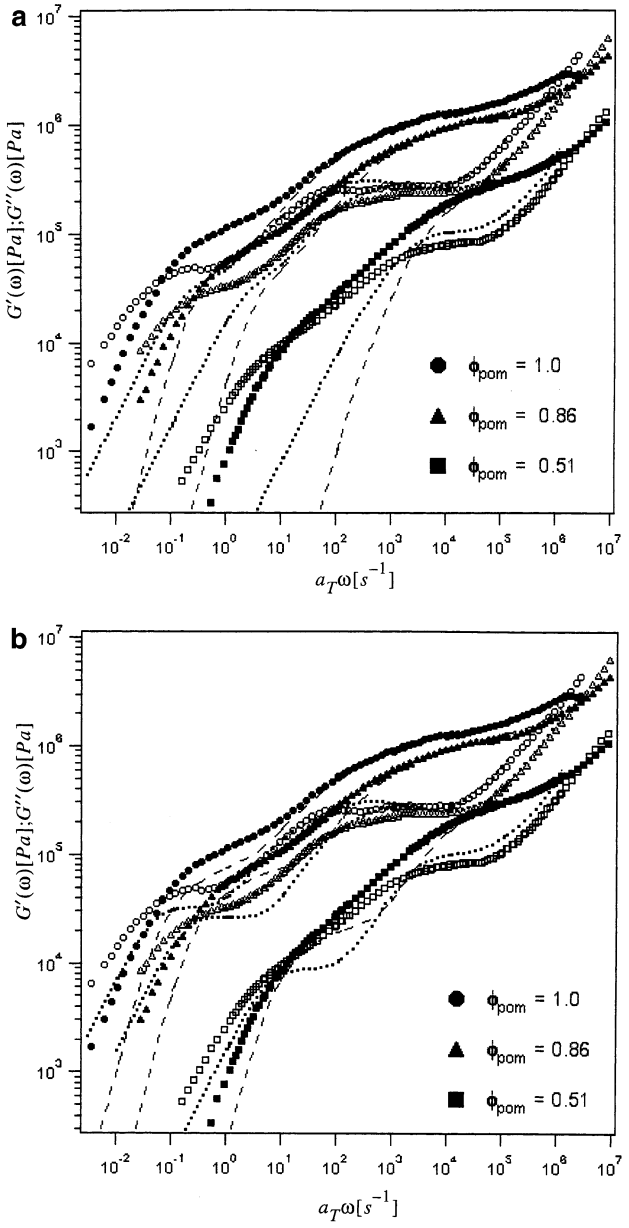

Figure 2. (**a**) Experimental $G'(\omega)$ (filled symbols) and $G''(\omega)$ (open symbols) for solutions of P1184 at 26 °C compared with theoretical predictions, $G'(\omega)$ (broken line) and $G''(\omega)$ (dots), for various solution concentrations. Theoretical results are for a fixed value of the branch point hopping parameter $p^2 = 1/6$. (**b**) $G'(\omega)$ (filled symbols) and $G''(\omega)$ (open symbols) for solutions of P1184 compared with theoretical predictions, $G'(\omega)$ (broken lines) and $G''(\omega)$ (dots), for various solution concentrations. Branch point hopping parameters $p^2 = 1/14$ in the melt, $p^2 = 1/35$ for a multiarm solution with $\phi_{pom} = 0.86$, and $p^2 = 1/110$ for a solution with $\phi_{pom} = 0.45$ were used in the analysis.

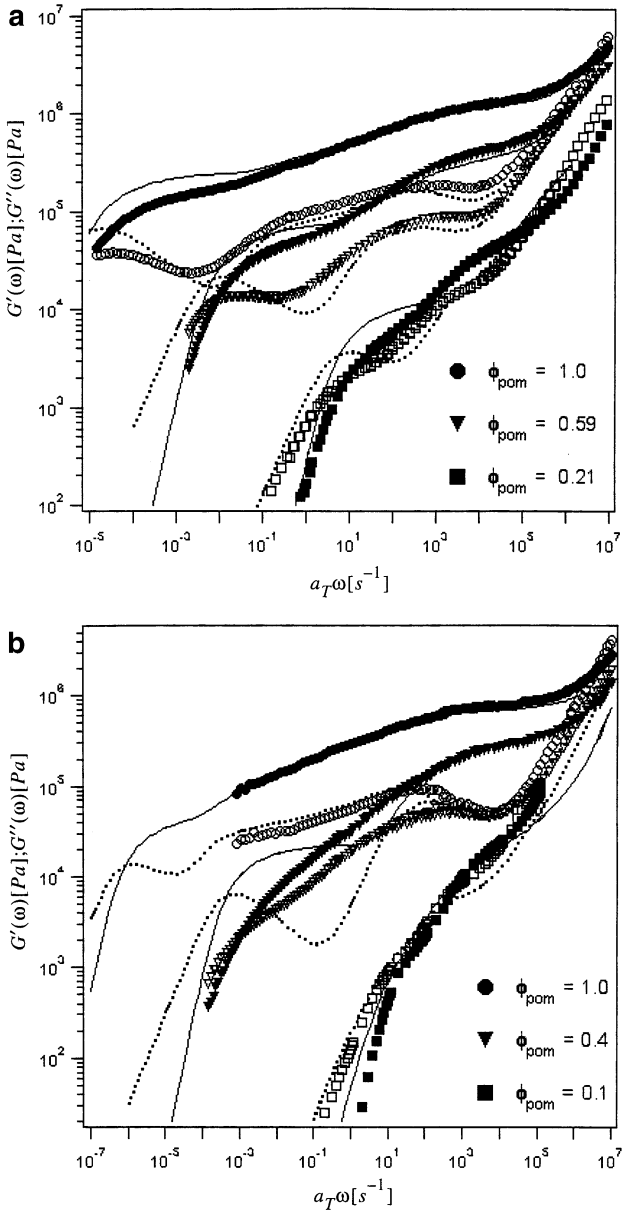

Figure 3. (**a**) Storage (filled symbols) and loss moduli (open symbols) for solutions of P1625 at 26 °C compared with theoretical predictions, $G'(\omega)$ (broken lines) and $G''(\omega)$ (dots), for various solution concentrations. Values of the branch point hopping parameter used in the analysis are provided in Table 4. (**b**) Storage (filled symbols) and loss moduli (open symbols) for solutions of MA15 at 26 °C compared with theoretical predictions, $G'(\omega)$ (broken lines) and $G''(\omega)$ (dots), for various solution concentrations. Values of the branch point hopping parameter used in the analysis are provided in Table 5.

Table 3. p^2 Values for P1184O_ Series Multiarm Solution

sample	ϕ_{P1184}	$1/p^2$	sample	ϕ_{P1184}	$1/p^2$
P1184O16	0.17	320	P1184O73	0.73	58
P1184O22	0.22	240	P1184O86	0.86	35
P1184O51	0.51	110	P1184	1.0	14

Table 4. p^2 Values for P1625O_ Series Multiarm Solution

sample	ϕ_{P1625}	$1/p^2$	sample	ϕ_{P1625}	$1/p^2$
P1625O10	0.1	330	P1625O59	0.59	42
P1625O20	0.21	190	P1625O83	0.82	18
P1625O38	0.38	154	P1625	1.0	26

ruled out architectural artifacts, unknown concentration dependence of segmental scale properties, and uncertainty of the dilution exponent as the source of these discrepancies.

In some cases, lower values p^2 significantly improve agreement between theory and experimental results. In other cases, unphysically low values of the parameter are required to achieve even qualitative correspondence between theoretical and experimental moduli. In fact, even in cases where moderate p^2 (i.e., $p^2 < 30$) are used to improve the theoretical predictions, branch points diffusion progresses in such small steps that terminal relaxation dynamics become dominated by arm retraction, which disagrees with the strict hierarchical process assumed in recent computer simulations. We believe that these results indicate that the influence of arm

Table 5. p^2 Values for MA15O_ Series Multiarm Solutions

sample	ϕ_{MA15}	$1/p^2$	sample	ϕ_{MA15}	$1/p^2$
MA15O080	0.08	250	MA15O30	0.31	3426
MA15O10	0.1	426	MA15O40	0.4	10426
MA15O20	0.2	226	MA15O50	0.5	9026

entanglements on $A_3-\mathbf{A}-A_3$ multiarm polymer dynamics are severely underestimated by theory. However, as shown in ref 1, these same polymers display clear evidence that relaxed arms enlarge the tube in which cross-bars relax. Taken together, the results seem to point to a fundamental difference between arm disentanglement (constraint release) and arm "disappearance" following relaxation. This finding is at odds with the dynamic tube dilation ansatz for stress relaxation in branched polymer liquids.

Acknowledgment. The authors are grateful to the National Science Foundation (Grant DMR9816105) for supporting this study. H NMR measurements were performed using facilities provided by the Cornell Center of Materials Research.

References and Notes

(1) Juliani; Archer, L. A. *Macromolecules* **2002**, *35*, 6953.
(2) Islam, M. T.; Juliani; Archer, L. A.; Varshney, S. K. *Macromolecules* **2001**, *34*, 6438.
(3) Ball, R. C.; McLeish, T. C. B. *Macromolecules* **1989**, *22*, 1911.
(4) McLeish, T. C. B. *Macromolecules* **1988**, *21*, 1062.
(5) McLeish, T. C. B.; Allgaier, J.; Bick, D. K.; Bishko, G.; Biswas, P.; Blackwell, R.; Blotteiere, B.; Clarke, N.; Gibbs, B.; Groves, D. J.; Hakiki, A.; Heenan, R. K.; Johnson, J. M.; Kant, R.; Read, D. J.; Young, R. N. *Macromolecules* **1999**, *32*, 6734.
(6) Larson, R. G. *Macromolecules* **2001**, *34*, 4556.
(7) Archer, L. A.; Varshney, S. K. *Macromolecules* **1998**, *31*, 6348.
(8) Ferry, J. D. *Viscoelastic Properties of Polymers*, 3rd ed.; Wiley: New York, 1980.
(9) Colby, R. H.; Rubinstein, M. *Macromolecules* **1990**, *23*, 2753.
(10) Daniels, D. R.; McLeish, T. C. B.; Crosby, B. J.; Young, R. N.; Fernyhough, C. M. *Macromolecules* **2001**, *34*, 7025.
(11) Daoud, M.; Cotton, J. P.; Farnoux, B.; Jannink, G.; Sarma, G.; Benoit, H.; Duplessix, R.; Picot, C.; deGennes, P.-G. *Macromolecules* **1975**, *8*, 804.

MA0208436